Cost Optimization Model for a Grid-Connected Offshore Wind and Tidal Power Generation System Using Homer: A Case Study in Buffels Bay South Africa

L. Kangaji[1*], A. Raji[1], E. Orumwese[2]
[1]Electrical Engineering, Peninsula University of Technology, Cape Town, 7535 2, South Africa
[2]Mechanical Engineering Department, Peninsula University of Technology, Cape Town, 7535 2, South Africa
[*]corresponding author's email: laskangaji@gmail.com

Abstract – *This study presents a cost optimization model for a grid-connected offshore wind and tidal power generation system, using Buffels Bay, South Africa, as a case study. The research utilizes the Hybrid Optimization Model for Electrical Renewable (HOMER) software to design and analyze a hybrid power system that integrates wind turbines, tidal energy, and battery storage with the local grid. Various system configurations were simulated to identify the most cost-effective solution, targeting the lowest Levelized Cost of Energy (LCOE) for a proposed 20 MW load. The optimized model combines tidal and wind power, contributing 62% and 20% of the total energy, respectively, demonstrating significant potential for renewable energy integration. The findings highlight the benefits of using a hybrid system to enhance reliability and reduce energy costs. Despite the low cost of coal-generated electricity in South Africa, the study shows that offshore wind and tidal energy can provide a sustainable and economically viable alternative, contributing significantly to the region's energy mix. This work offers valuable insights for future renewable energy projects in coastal regions with similar environmental and economic conditions.*

Keywords*: grid-connected, HOMER Pro, microgrid, tidal energy, wind energy*

Article History
Received 14 September 2024
Received in revised form 29 October 2024
Accepted 3 December 2024

I. Introduction

In 2008, South Africa was confronted with a stark reality; the constitutional promise of secure and sustainable electricity access could not be met. The country, which depends on non-renewable fossil fuels for over 95% of its electricity, experienced a peak and subsequent decline in these resources [1]. The remaining coal is either inexpensive but low-quality surface coal or costly high-quality deep-level coal [2]. As a result, the cost of electricity generation is rising to meet increasing demand, further escalating prices. Notably, 20% of this demand originates from the domestic housing sector [3]. Electricity generation, primarily dependent on coal, gas, and oil, significantly contributes to global warming through substantial greenhouse gas emissions [4]. The ongoing conflict between Russia and Ukraine has exacerbated this issue, causing a sharp rise in fossil fuel prices [5]. Conversely, electricity generated from secure, sustainable, and renewable sources could greatly promote sustainable development, economic growth, and climate change mitigation [3]. For example, implementing a 50 kWh/month solar system for low-cost housing could save the country over R100 billion annually and reduce national grid electricity consumption by 9,720 GWh per year, equivalent to 5.8million tonnes of CO_2 [6]. Renewable energy sources, such as tidal energy, are widely recognized for being clean, natural, and abundant, making them essential for advancing sustainable development. These resources are particularly crucial for coastal cities and villages with limited electricity access. To improve the efficiency and reliability of tidal stream turbine systems, distributed energy storage devices like electrolysers, super capacitors, hydrogen banks, and batteries have been integrated. These technologies effectively manage excess power and address energy deficits [7]. Despite these advances, offshore wind power faces challenges, notably its high cost, approximately double that of onshore wind power [8]. Moreover, relying solely on offshore wind power results in significant output fluctuations and poor predictability, necessitating careful consideration of its integration into the grid [9]. In contrast, tidal current energy demonstrates more predictable periodic output fluctuations, highlighting its success as an application of ocean energy [10]. While many planned wind farms are

located in areas with water depths exceeding 30 meters, where traditional support structures may no longer be feasible, resulting in higher capital costs for the necessary systems. Consequently, the levelized cost of energy is likely to remain higher than that of gas or coal generation, making large-scale wind deployment dependent on ongoing government incentives [11].

To reduce electricity generation costs, co-locating wind farms with other renewable technologies has been proposed. Consequently, there is growing interest in combining offshore wind power with tidal current power generation systems. [12]–[14] et al. proposed an innovative combined generation approach integrating offshore tidal current and wind power to effectively manage system costs .

This study examines the co-location of offshore wind turbines with tidal stream turbine farms. Although tidal stream turbines are less mature than offshore wind or solar technologies, tidal arrays are currently being installed. The UK, for example, has the potential to generate an estimated 18 TWh/year from tidal stream resources, with the Pentland Firth alone capable of providing over 2 GW of average power. Co-location offers advantages such as shared electrical infrastructure and potentially shared support structures [15]. Additionally, co-located farms may experience reduced power variability compared to operating wind or tidal farms independently. Existing offshore wind farms have typically been established in areas with low tidal stream velocities [16]. Furthermore, extensive research has been directed towards enhancing the competitiveness of tidal energy, including its integration with other renewable sources and optimizing performance through combined use with wind turbines and storage [17].The inception of offshore wind power projects, initially driven by onshore wind power developments, began early in their research and development stages [8].

Globally, grid-connected systems of this type have gained widespread adoption, particularly in smart city initiatives. Techno-economic analyses have consistently shown the feasibility of both standalone and grid-connected hybrid energy systems [18]. While many studies have utilized tools like HOMER for renewable energy simulations, this study represents the inaugural application of HOMER Grid in simulating a grid-connected system for a public institution. A significant barrier impeding South Africa's broader adoption of renewable energy is the lack of critical mass among society and government regarding commercial electricity generation from renewable sources. Therefore, this study aims to conduct a techno-economic analysis and optimization of a campus grid-connected tidal–wind turbine system using HOMER pro Grid. Its goal is to cultivate critical mass from grassroots levels of society and future generations. This study focuses on optimizing the cost of a grid-connected offshore wind and tidal power generation system using HOMER pro software, with a case study in Buffels Bay, South Africa. The primary objective of this paper is to assess the economic feasibility of a hybrid power system that integrates both tidal and wind turbines to meet the specific load requirements of the area. For comparison, an off-grid hybrid power system that incorporates tidal, wind, and battery storage is also designed. The paper is structured as follows: section II provides a detailed description of the system model, section III outlines the methodology, section IV presents the simulation models used, section V analyzes the optimization results and section VI concludes the findings.

II. Literature Review

This research facilitates the selection of the optimal hybrid tidal-wind energy system for a coastal city by incorporating specialized displays along with environmental and economic considerations [19]. A highly practical and reliable alternative to conventional power grids for electrifying rural regions is the Hybrid Renewable Energy System (HRES).They play a crucial role in reducing fossil fuel consumption and mitigating climate change [20]. HRES offer several advantages over single-energy-source systems, including enhanced reliability, decreased energy storage requirements, improved efficiency, modularity, and a lower Levelized Cost of Energy (LCOE)[21].This systematic literature review delves into various configurations and optimization strategies for hybrid renewable energy systems (HRESs), focusing on developments from 2015 to 2024. Solar energy, characterized by its intermittent nature, often necessitates energy storage (ES) systems to mitigate supply and demand fluctuations in [22]. Similarly, wind turbines can effectively utilize ES units such as batteries to stabilize power output and store excess energy in [23]. Studies, such as those by Ghayoor [24], have explored the feasibility of small-scale wind turbines for consumers in Africa [25]. As Sanedi, et al., (2017) [2] argue that solar-ES configurations are more advantageous than wind-ES due to wind speed variability, although contrasting findings by Maleki et al. [26] underscore the regional variability in hybrid system resource selection based on meteorological conditions and load characteristics.

Another effective configuration is the wind-solar-energy storage (wind-solar-ES) system, which leverages the complementary characteristics of wind and solar energy to enhance system reliability and minimize storage requirements.

Hybrid Renewable Energy Systems (HRES) enhance the overall stability and reliability of energy generation by effectively addressing the intermittency issues of individual renewable sources. Solar energy is most productive during the day, while wind energy can be harnessed even when sunlight is minimal [26].

Integrating diverse energy resources enhances the reliability of the energy supply, decreasing the risk of blackouts during adverse weather conditions. Furthermore, the incorporation of energy storage technologies within hybrid systems enables the capture of excess energy produced during peak output periods. This stored energy can subsequently be utilized during times of lower generation, thereby improving overall system efficiency and reducing energy wastage [18].

Standalone renewable energy sources are intermittent, which can place stress on existing power systems, resulting in voltage and frequency fluctuations. The integration of hybrid systems with energy storage capabilities helps manage these fluctuations more effectively, allowing excess energy to be supplied to the grid during peak demand periods. This approach improves grid stability and mitigates congestion, facilitating a smoother integration of renewable energy into current power infrastructures [6].

The optimal design of hybrid renewable energy systems (HRES) is a well-researched topic, and extensive literature is available. The design problem involves determining the best configuration of the power system and the optimal location, type, and sizing of generation units to meet load requirements at minimal cost [27]–[29]. Optimal sizing remains crucial in HRES design, aiming to achieve desired reliability at minimal costs [30]. Objective functions encompass economic, reliability, social, and environmental aspects, driving the use of optimization tools ranging from classical techniques to modern meta-heuristic algorithms like Genetic Algorithms (GA) and Particle Swarm Optimization (PSO) [31]-[32]. The evolution of these methodologies from 2015 to 2024 highlights advancements in overcoming local optima and improving convergence efficiency in complex HRES sizing problems. Widely adopted software tools such as Hybrid Optimization Model for Electric Renewables (HOMER) and Improved Hybrid Optimization by Genetic Algorithm (iHOGA) continue to play a pivotal role in optimizing HRES configurations [14].

Ssennoga et al.,(2018)[33] provided statistical modeling of solar-wind HRES based on annual cost, battery autonomy, sizing criteria, and ecological factors, employing step-by-step optimization to achieve optimal results. Hirose et al.,(2012) [34] developed a solar-wind hybrid system model incorporating diesel generators with renewable energy sources, based on long-term simulations. Modu [35] presented a logistical model of HRES to evaluate fuel and energy savings, addressing issues related to combining renewable and conventional energy sources. This model introduces a supplementary fictitious source to maintain power balance during simulations.

Suchitra et al., (2019) [36] used the loss of power supply probability (LPSP) to develop an integrated renewable energy system model, deriving the probability density function of the storage based on load distribution. Simulation programs are widely used to evaluate the performance of HRES, with many available for download from research laboratories and universities [37]. These programs help find the optimal configuration by comparing different system setups' performance and energy production costs. The National Renewable Energy Laboratory (NREL) in the United States is recognized for developing the widely respected HOMER software. HOMER models various energy components, including photovoltaics (PV), tidal stream turbines, wind turbines, hydropower, batteries, diesel generators, and other fuel-based generators, as well as electrolysis units and fuel cells. It also evaluates optimal solutions by considering both costs and the availability of energy resources.

III. Methodology

A. Tidal Stream Turbine

The objective of the tidal stream turbine (TST), as shown in Fig. 1, is to maximize power extraction from the wind or tidal flow. The following equations describe the torque produced by the turbine rotor and the power transferred to it.

$$P_t = C_p P_{flow} = \frac{1}{2} A V_{flow}{}^3 C_p(\beta, \lambda) \quad (1)$$

$$T_t = \frac{P_t}{\omega_{rot}} \quad (2)$$

where P_{flow} (W) represents the power of the air or tidal stream flow, as illustrated in Fig. 2. The fluid density is 1025 kg/m^3. A (m^2) denotes the rotor's swept area, V_{flow} (m/s) is the upwind free wind speed or tidal stream flow speed, C_p is the power coefficient, and ω_{rot} (rad/s) represents the rotor's angular speed [16]. Table II details the tidal parameters.

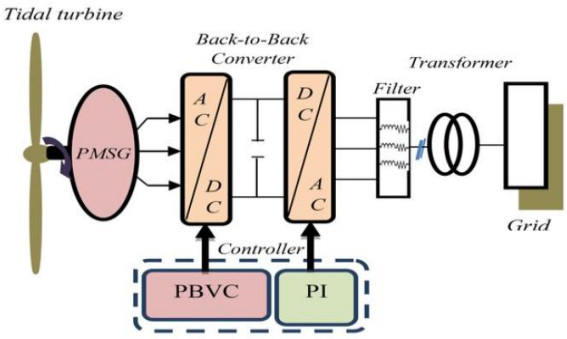

Fig.1.Tidal energy systems configuration based on a PMSG [38]

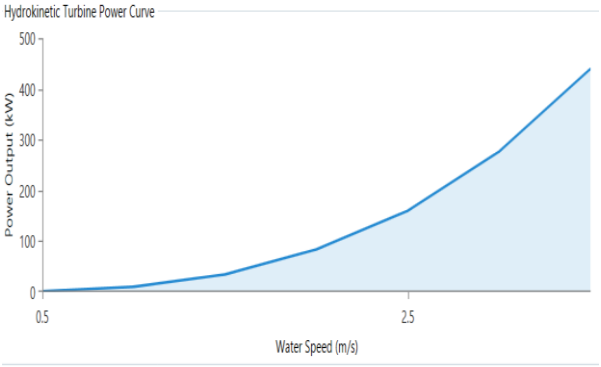

Fig.2. Power Output Curve for the Schottel 54 kW Tidal Turbine

TABLE I
TIDAL PARAMETERS

Parameters	Symbols	Values
Cut-in tidal speed	v_{cuttid}	< 1 (m/s)
Rated tidal speed	$v_{ratedtid}$	3 m/s
The cross-sectional area of turbine	A	201.06 m^2
Power coefficient	C_p	0.44
Cut-out tidal speed	$v_{cututtid}$	>5 m/s

B. *Tidal Stream Turbine*

Fig. 3 illustrates a wind energy conversion system. The wind turbine converts wind kinetic energy into AC or DC electricity based on its power curve, and HOMER estimates the turbine's hourly electricity production through a four-step process [7].

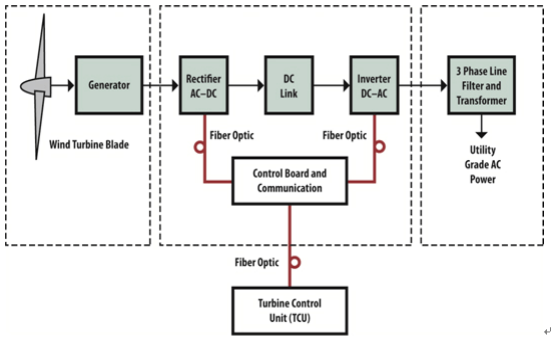

Fig. 3. Block diagram illustrating the components of a wind energy conversion system [39]

The process begins by determining the hourly average wind speed using wind resource data, which is then adjusted to the turbine's hub height using logarithmic or power-law equations. Next, the power output is calculated based on the turbine's power curve, and this output is further adjusted by considering the air density ratio. HOMER uses the power-law formula to extrapolate wind speed data [40].

$$U_{hub} = U_{anem}\left(\frac{Z_{hub}}{Z_{anem}}\right)^{\alpha} \quad (4)$$

Wind turbine performance is usually defined by power curves under standard conditions. HOMER adjusts the power output by applying the actual air density ratio to the estimated power value from the curve, which assumes an air density of 1.225 kg/m³.

$$P_{WTG} = \left(\frac{\rho}{\rho_o}\right) XP_{WTG,STP} \quad (5)$$

The power coefficient of a wind turbine is influenced by both the tip-speed ratio (TSR) and the blade pitch angle. Fig. 4 presents the typical variation of the power coefficient as a function of TSR for various pitch angles (β).

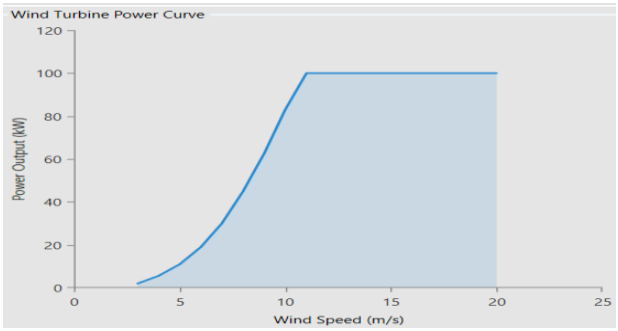

Fig.3. Power generation distribution for the XANT M-21 turbine

The E-70 wind turbine is utilized in this study, with key parameters outlined in Table II.

TABLE II
WIND TURBINE PARAMETERS

Parameters	Symbols	Values
Cut-in wind speed	v_{cuttid}	5 m/s
Rated wind speed	$v_{ratedtid}$	15 m/s
The cross-sectional area of turbine	A	3959 m^2
Power coefficient	C_p	0.44
Cut-out tidal speed	$v_{cututtid}$	25 m/s
The maximum output power	P_{wmax}	2300 W
Rotor diameter		71 m
Hub height		25 m and 100 m

C. *Battery Sizing*

HOMER models a single battery as having fixed energy efficiency, with constraints on charging and discharging rates and total energy throughput. The software assumes that battery characteristics remain constant over time and

are unaffected by environmental conditions. A battery bank, consisting of one or more batteries, has its lifespan calculated using a specific equation [41].

A battery is an energy source when discharging and a load when charging. Energy is stored in the batteries when the power generated by the tidal or wind turbine exceeds the load demand. A battery serves as an energy source when discharging and as a load when charging. It stores energy when the power output from tidal or wind turbines exceeds the load demand. Conversely, it supplies energy when the generated power is insufficient. The state of charge (SOC) is used to control charging and discharging. When SOC reaches its maximum value, the control system disconnects the load to prevent overcharging. In an integrated renewable energy system, batteries have two main functions: storing excess energy during charging and providing additional energy to meet load demands. If SOC drops to a minimum level, the control system adjusts to manage the excess power and ensure that the load's energy needs are met. Mathematically, this is expressed by maintaining SOC above a minimum level throughout any cumulative time t within a specified period T [42].

$$R_{bat} = MIN\left(\frac{N_{bat} \times Q_{lifetime}}{Q_{thrpt}}, R_{batt,f}\right) \quad (6)$$

where R_{bat} represents the lifespan of the battery bank (in years), N_{bat} is the number of batteries in the storage bank, $Q_{lifetime}$ is the total energy throughput of a single battery over its lifetime (in kWh), Q_{thrpt} is the annual energy throughput of the storage system (in kWh/year) and $R_{batt,f}$ is the float life of the storage system (in years) [42].

D. Sizing Procedure Based on Supply Reliability

Supply reliability is a key factor in designing an integrated tidal/wind-battery system and influences various sizing procedures. It refers to the probability that the power system will operate correctly over a specified period under given conditions without failure. This study presents a program for optimizing the sizing of components in the integrated energy system (tidal and wind-battery) by assessing generation adequacy through a reliability index. The Loss-of-Power Supply Probability (LPSP) parameter is one method used to quantify supply reliability [43] as in (7).

$$LPSP = P_r(E_B(t) \leq E_{Bmin}; for\ t \leq T) \quad (7)$$

E. Converter

A converter is a device that converts electrical power from DC to AC during inversion and from AC to DC during rectification. HOMER models both solid-state and rotary converters. The size of the converter is determined by its inverter capacity, which indicates the maximum AC power that can be produced from DC electricity. The rectifier capacity, expressed as a percentage of the inverter capacity, denotes the maximum DC power that can be generated from AC power, making it a dependent variable. HOMER assumes that both inverter and rectifier capacities are continuous and free from surges, ensuring stable load management. The inverter can operate in parallel with other AC power sources, such as a generator or the grid. The inverter can operate in parallel with other AC power sources, such as generators or the grid. HOMER assumes that the key physical attributes of the converter, including inversion and rectification efficiencies, remain constant. The economic characteristics of the converter include capital cost, operation and maintenance (O&M) costs, replacement costs, and expected lifespan, all expressed in US dollars per year [44].

F. Economic Analysis

Conducting a techno-economic analysis of an engineering system requires specific economic data, including the nominal discount rate, expected inflation rate, and project lifetime. The necessary economic data for this analysis are presented in Table III.

1. Net Present Value (NPV)

$$NPV = \sum_{t-0}^{n} \frac{C_t}{(1+r)^t} \quad (8)$$

where C_t is Net cash flow at time *t*, r is the nominal discount rate and n is the project lifetime.

2. Main Internal Rate of Return (IRR)

The IRR is the discount rate *r* at which the NPV equals zero.

$$\sum_{t-0}^{n} \frac{C_t}{(1+IRR)^t} = 0 \quad (9)$$

3. Levelized Cost of Energy (LCOE)

$$LCOE = \frac{\sum_{t=o}^{n} \frac{C_t}{(1+r)^t}}{\sum_{t=0}^{n} \frac{E_t}{(1+r)^t}} \quad (10)$$

where E_t is the energy generated at time t.

4. Simple Payback Period

$$Payback\ Period = \frac{Initial\ Investment}{Annual\ Net\ Cash\ Flow} \quad (11)$$

5. Annualized Cost

$$Annualized\ Cost = \frac{C_{total}.r.(1+r)^n}{(1+r)^n-1} \quad (12)$$

6. Salvage Value

$$Salvage\ Value = C_{initial}.\left(\frac{R_{rem}}{R_{total}}\right) \quad (13)$$

where $C_{initial}$ is initial capital cost, R_{rem} is the remaining life of the component and R_{total} is the total expected life of the component.

7. Loss-of-Power Supply Probability (LPSP)

$$LPSP = \frac{\sum_{t=0}^{n} Power\ Defit_t}{\sum_{t=0}^{n} Load\ Demand_t} \quad (14)$$

where *Power Deficit*$_t$ is power deficit at time *t* and *Load Demand*$_t$ is the load demand at time *t*.

8. Discount Factor

$$DF_t = \frac{1}{(1+r)^t} \quad (15)$$

where DF_t is discount factor at time *t*.

9. Cost of Energy (COE)

$$COE = \frac{Total\ Annualized\ Cost}{Total\ Annual\ Energy\ Production} \quad (16)$$

10. Simple Payback

The simple payback period is defined as the number of years required for the cumulative cash flow difference between the optimized and reference case systems to transition from negative to positive. This metric indicates the time needed to recover the initial investment cost difference between the optimized system and the reference system.

11. Total Annualized Cost

The total annualized cost of a component is the uniform annual expense that, over the project's lifespan, equates to the net present cost of the component's actual cash flows. This cost is calculated by multiplying the net present cost by the capital recovery factor, as indicated in the following equation.

$$C_{ann,tot} = CRF\left(i, R_{proj}\right) \times C_{NPC,tot} \quad (17)$$

where $CRF(I, R_{proj})$ is the capital recovery factor, i is the discount rate, R_{proj} is the project lifetime and $C_{NPC,tot}$ is the total net present cost.

12. Emissions Reduction

The reduction in emissions is determined by the amount of energy generated by the renewable energy system, which replaces the energy that would otherwise be produced from fossil fuels. This reduction is expressed as emissions per unit of energy consumed. The emission data used for these calculations are detailed in Table IV. By applying these formulas, HOMER evaluates the economic performance of the integrated energy system, enabling comprehensive techno-economic analysis and informed decision-making.

G. System Description

The primary objective of this study is to develop a cost-optimization model for a grid-connected hybrid energy system using HOMER Pro software. The model seeks to identify the optimal configuration that minimizes costs while ensuring a reliable power supply for a local coastal community in South Africa. This paper involves designing both on-grid offshore hybrid power systems using HOMER software to assess and determine the costs associated with various configurations. Specific input data is required for the HOMER simulation software to evaluate optimization outcomes across different combinations, as detailed in the subsequent section.

The proposed hybrid system in HOMER software involves determining the load profile of a remote area, acquiring meteorological data for solar irradiance and hydroflow rates, and configuring the system components. Economic parameters and component sizes are established, and simulations are conducted for cost optimization. The levelized cost of energy (LCOE) is evaluated to ensure that the selected solution meets the study's objectives. HOMER ranks the results based on cost, with the most optimized solution being the one with the lowest Net Present Value (NPV). Fig. 5 shows the steps of the model in HOMER.

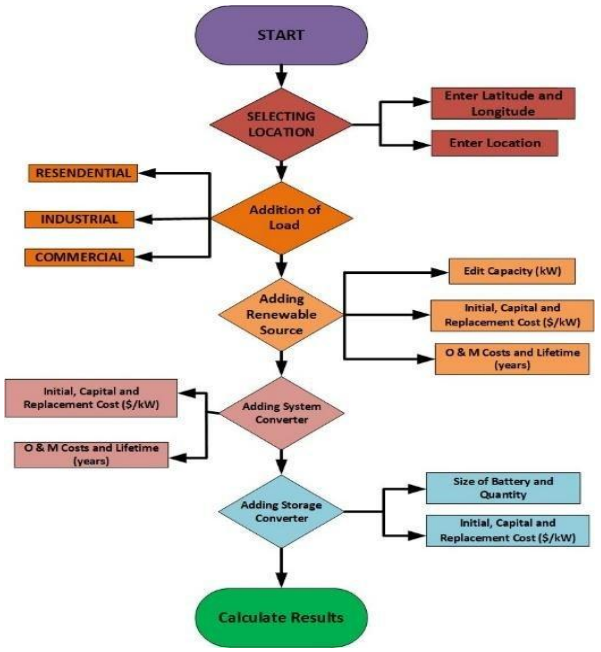

Fig.4. Steps of the model in HOMER

Whether the choice of selected result fulfils the objective of this work. HOMER ranked its result based on the least cost combination. The most optimized result by mean is the most optimal solution which is at the lowest cost of Net Present Value (NPC).

H. Site Selection

Buffels Bay, 657, South Africa (34º5.1′S,2258.2′E), was chosen as a case study to assess the feasibility of a hybrid system combining wind and tidal turbines connected to a microgrid to supply power to remote coastal communities isolated from the national grid. Buffels Bay is a small seaside village located 20 kilometres from Knysna as shown in Fig. 6, within the Garden Route District Municipality in South Africa's Western Cape province. The village is named after the nearby bay that extends eastward.

It is a well-known vacation spot, featuring a small waterfront area with shops. This area, a small tourist destination near Cape Town, experiences unstable electricity access due to load shedding by ESKOM in Fig. 7. Currently, the community relies on a diesel power station located in the island's main settlement for electricity.

Ongoing research at the Centre for Renewable and Sustainable Energy Studies CRSES is examining the relationship between diesel usage and load shedding as indicated in Fig. 7. In the meantime, these two metrics are presented together for comparison [6].

- Optimizing the design involves identifying the optimal location, and size of devices required to harness these energy resources.
- Conducting a feasibility analysis and assessing the financial viability of the optimized microgrid design.

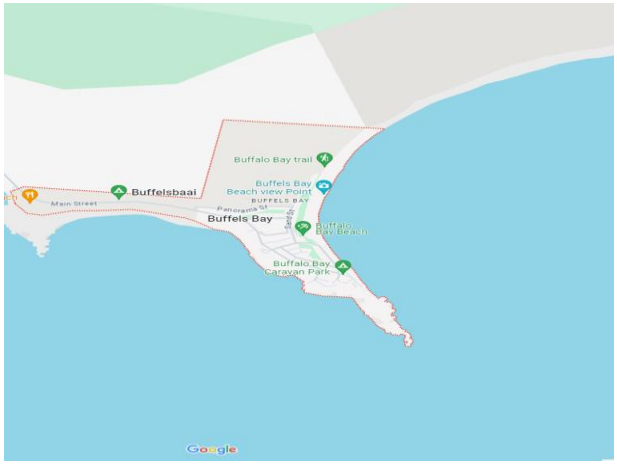

Fig. 6.Buffels Bay is a small seaside village location

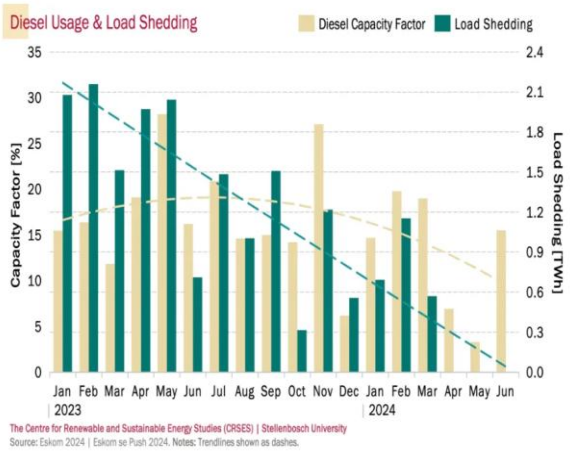

Fig.7.The relationship between diesel consumption and load shedding [6]

I. Data Collection

The east coast of South Africa, as illustrated in Fig. 8, features current flows that make this region suitable for potential tidal farm locations. To ensure economic viability, a stream velocity of at least 2 m/s is necessary for a tidal farm. This study, therefore, proposes a tidal Stream Energy conversion system. Buffels Bay has been identified as a promising site based on tidal data from the South African Navy Hydrographic Office (SANHO) [45].

Fig. 9 illustrates an example of the fortnightly spring-neap water level cycle observed at Mossel Bay. Similar to the conditions in Mozambique, the spring-neap cycle and daily inequality are significant along the South African

coast. Mean High Water Spring (MHWS) refers to the annual average height of high-water during spring tide periods, relative to Chart Datum. This average is calculated once every fortnight. The difference between MHWS and Mean Low Water Spring (MLWS) can also be considered the Mean Spring Tide Range (MSR), which is approximately 1.5 meters along the South African coastline [46].

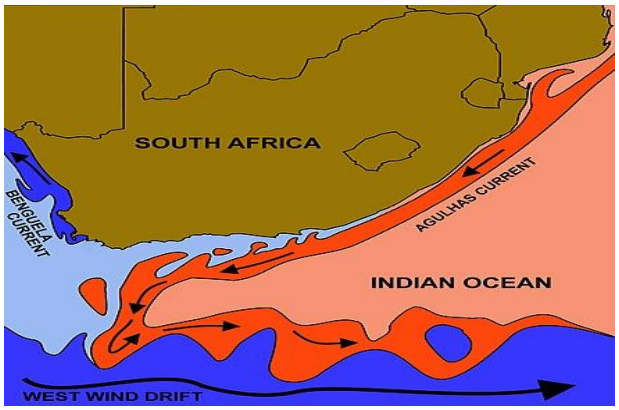

Fig. 5. Agulhas Currents systems [45]

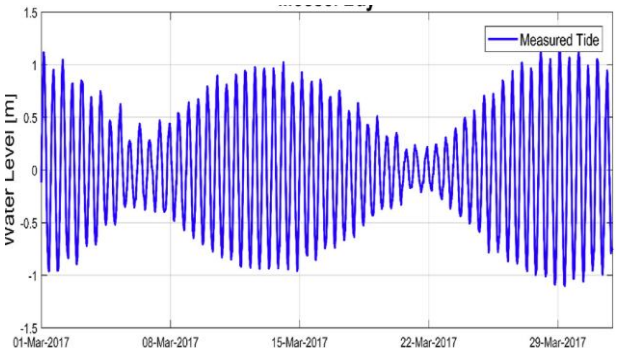

Fig.6. Tidal water levels were measured over two spring tide cycles, emphasizing the significance of the tidal cycle [46]

Wind speed and community load demand data for Buffels Bay, South Africa, were gathered from local meteorological stations and historical records.

This study evaluated seven sites in Cape Town, South Africa - Cape Town with their geographical locations are shown in Fig. 10. Hourly mean wind speed data from 2000 to 2019 as shown in Fig. 11, measured at 10 meters above ground level, were analyzed to identify the most suitable sites for wind power development. The wind speed data were extrapolated to various heights using a power law with a wind shear exponent of 0.14. The analysis covered annual, monthly, and diurnal variations in wind speed. Factors such as annual energy yield, plant capacity, and power duration were assessed to recommend the best sites and wind turbines. Key findings include:

- Port Elizabeth recorded the highest mean wind speed at 6.01 m/s, while Bloemfontein had the lowest at 3.86 m/s.
- Coastal sites (Cape Town, Durban, East London, and Port Elizabeth) showed an increasing trend in wind speed with higher latitudes [47].

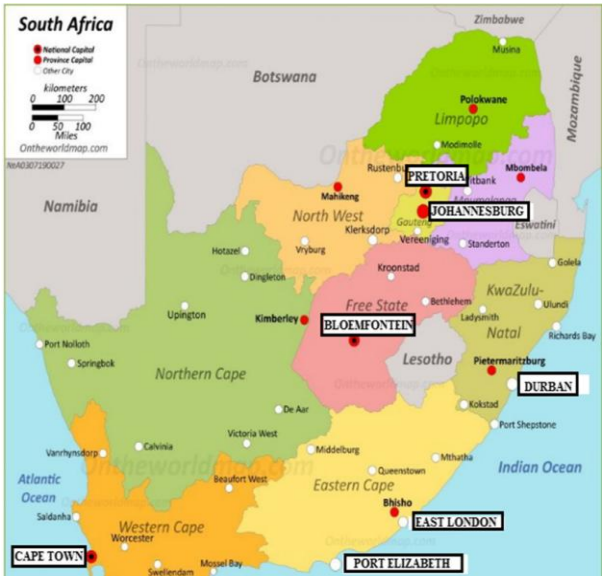

Fig.7.Coastal sites

The data, typically provided in hourly, daily, or monthly time series, was imported into HOMER using meteorological databases, local weather stations, and NASA's Surface Meteorology and Solar Energy (SSE) database. Additionally, tidal data for Buffels Bay was obtained from the Tide Forecast website, including specific tide conditions and charts for East London and Cape Town. Fig. 12 shows the monthly average micr-hydro resources.

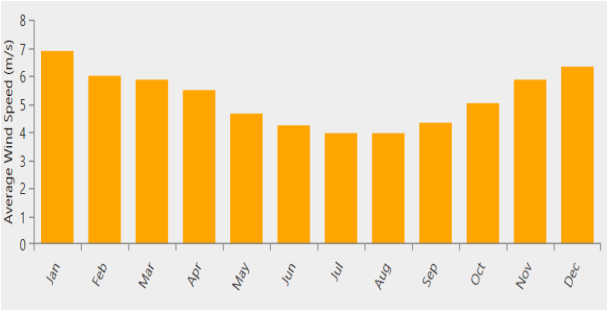

Fig. 8. Monthly Average Wind Speed

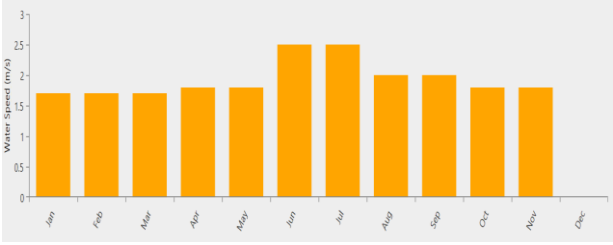

Fig. 9. Monthly Average Micro-Hydro Resouces

The village, which currently lacks historical electrical load data due to its non-electrified status, estimates its electrical load through assumptions. For a case study involved, the peak demand is estimated at 4500 kW, with an 80% load diversification applied to the base load without accounting for area-specific variations. The village is connected to the Buffels Bay customer load network and uses a scaled-down version of the demand profile, peaking at approximately 597 kWh to project its own demand. Detailed load data is recorded hourly, covering a full year (8760 hours), and is used as input for HOMER Pro®. The load primarily consists of residential properties, showing two distinct peaks: a smaller one in the morning and a larger one in the evening. Fig. 13 illustrates the average hourly loads throughout the year, while Fig. 14 shows the yearly average loads, indicating higher demand during the winter months (June-August) [40].

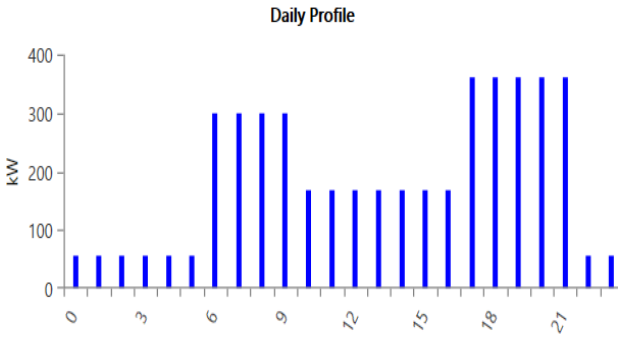

Fig.10.Variation of load demand for 24 hours

Fig. 14 illustrates the seasonal variations in electricity demand for the West Bank community. Generally, demand rises during the colder months due to greater heating requirements and may also increase during hot summer months if air conditioning is commonly used. This profile highlights the fluctuations in electricity consumption, showcasing the community's usage patterns in response to seasonal changes.

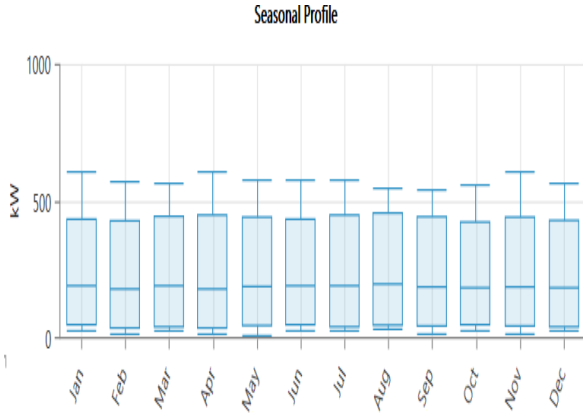

Fig.11. Seasonal profile of load demand throughout the year

A study by Prinsloo and Davidson found that in an African village, the average household consumes about 12.5 kW, with usage peaks between 9:00-11:00 and 15:00-18:00. Lighting is used from 18:00 to 23:00, and appliances such as a radio (5W) and a TV (70W) are typically operated during this time. To address a 20 MW load demand throughout the day, typical consumption patterns across residential, commercial, industrial, and public service sectors will be considered. This detailed daily load profile is based on a total demand of 20 MW. The data shows peak demand in June (69.29 kW) and between 6:00-7:00 PM (69.29 kW), with the lowest demand in January (162 kW) and between 3:00-4:00 PM (37 kW) [48].

J. Proposed System Architecture

Fig. 15 depicts the circuit model of a Hybrid Offshore Tidal Turbine (HOTT) system integrated with a battery [13]. In this setup, the output of the induction generator connected to the tidal turbine can be modulated to stabilize frequency and manage active power fluctuations [12].

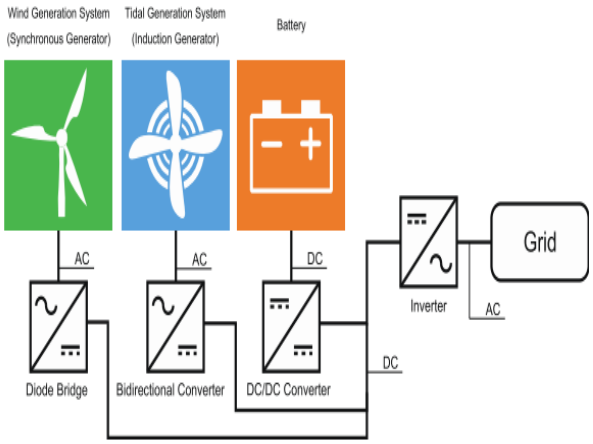

Fig. 12. Conceptual System Schematic of HOTT with Battery [49]

Before simulating the renewable energy system,

designing the system architecture is essential. This design includes lead-acid batteries and a converter for energy storage, supported by power sources like tidal and wind turbines. For tidal energy, the Schottel 54 kW bidirectional turbine was selected due to its low cut-in speed, ability to meet peak load demands, and cost-effectiveness in purchase, installation, and maintenance.

The turbine's costs are $54,000 for capital and replacement, $2,700 annually for maintenance, and it has an operational lifespan of 10 years. The proposed wind turbine has a capacity of 100 kW, a hub height of 31.80 meters, and an operational lifespan of 25 years.

Energy storage is managed by lead-acid batteries, each with a nominal voltage of 12 V, a nominal capacity of 1 kWh, a capacity ratio of 0.403, a roundtrip efficiency of 80%, a maximum state of charge of 100%, a minimum state of charge of 40%, a throughput of 800 kWh, and a lifespan of 10 years.

The system's converter has a capacity of 100%, with inverter and rectifier efficiencies of 95%, and a lifespan of 15 years. All equipment specifications were sourced from the software's catalogue. Fig. 16 provides a schematic diagram of the proposed system architecture, with detailed specifications in Table III. A DC bus interconnects all components, with wind and tidal turbines as the primary energy sources.

In HOMER, selecting the appropriate load profile for residential, commercial, industrial, or community is crucial. For this study, a residential load profile was chosen. When energy storage is included, HOMER requires specifying the storage type.

To ensure the proposed microgrid can operate independently, the ion lithium battery was selected for energy storage after extensive simulations [14]. The grid-connected system integrates wind and tidal turbines with a battery energy storage system (BESS) to compensate for periods with insufficient wind and tidal currents [50].

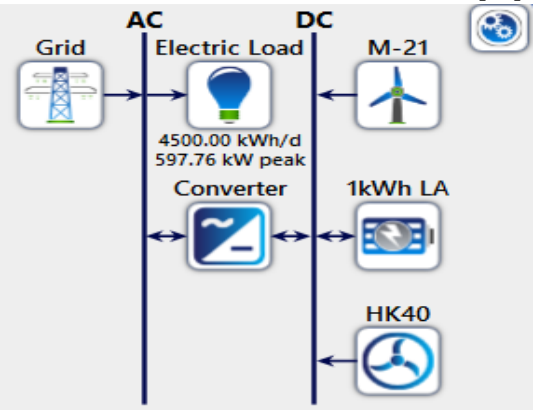

Fig. 13. Proposed system architecture

IV. Results and Discussion

Table IV displays the comprehensive results of the cost optimization analysis, ranked in descending order. In this study, the selected configuration is on the third line, comprising The XANT M-21 (100 kW) and Schottel (54 kW) turbines are efficient for meeting peak load demands with low costs. The XANT M-21 has capital and replacement costs of $50,000 each, maintenance costs of $2,500/year, and a lifespan of 20 years.

The Schottel turbine costs $54,000 for capital and replacement, $2,700/year for maintenance, and has a 10-year lifespan. Additionally, a generic 12-volt lead–acid battery offers reliable performance with capital and replacement costs of $154 each, $15.40/year for maintenance, and a 10-year lifespan.

TABLE III
NET PRESENT COSTS

Component	Name	Capital Cost (USD)	Replacement	O&M Cost (USD)	Lifetime	Ref
Grid	ESKOM					[24]
Tidal turbine	(Schottel, Spray, Germany) (54 kW)	$54,000.00	$54,000.00	$2700/year	10 years	[51]
Wind turbine	XANTM21	210,000.00	210,000.00	3500/year	25 years	[14]
Storage	1 kWh Lead Acid	300/kW	300/kW	25/year	10 years	[52]
Converter	System Converter	300/kW	300/kW	0	15 years	[53]
Controller		$200.00	$200.00	0		[54]

TABLE IV
ANNUALIZED COSTS

Component	Capital ($)	Replacement ($)	0&M ($)	Fuel ($)	Savage ($)	Total ($)

Gen Hydro (40kw)	$70,000.00	$60,913.97	$0.00	$0.00	$8,154.95	$122,759.01
Grid	$0.00	$0.00	$816,533.04	$0.00	$0.00	$816,533.04
System Converter	$59,003.14	$24,619.95	$0.00	$0.00	$4,582.55	$79,040.54
XANT M-21 (100KW)	$300,000.00	$77,951.18	$127,833.56	$0.00	$43,68687.24	$462,097.50
System	$429,003.14	$163,485.10	$944,366.60	$0.00	$56,424.75	$1,480,430.09

The inflation rate was set at 5.2% (South Africa), with a discount rate of 0%. Two primary tests were conducted in this study. This section investigates multiple scenarios to assess how the grid electricity purchase and sellback prices (Grid power price/Grid sellback price) affect the financial returns of renewable energy investments over a 25-year period.

Resources are external parameters essential for HOMER in microgrid system analysis. The choice of these resources, which depends on the location, directly impacts both power generation and the financial feasibility of the microgrid design. Therefore, selecting the right resources is crucial for an effective analysis. For this microgrid design, the key resources are wind speed data (sourced from NASA) and water speed data (obtained from https://www.tide-forecast.com) for the year 2024. Fig. 17. shows the power generation potential of the wind and tidal turbines at the Buffels Bay site based on this data.

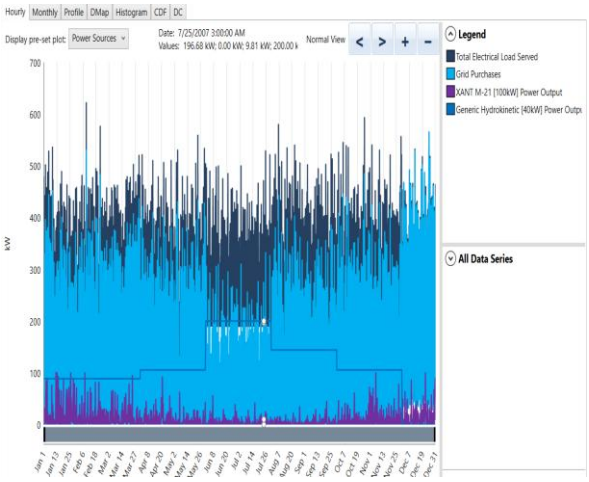

Fig. 14. Variations in power output for tidal turbines and wind turbines at the Buffels Bay site

A. Power Generation Results

Figs. 18(a) – (b) illustrates the monthly average power output (kW) and resource distribution for various scenarios. The renewable energy share for the wind-only scenario (36 kW) is 66.3%, which exceeds that of the tidal-only scenario (63.9%) and the combined wind and tidal sources (65.4%).

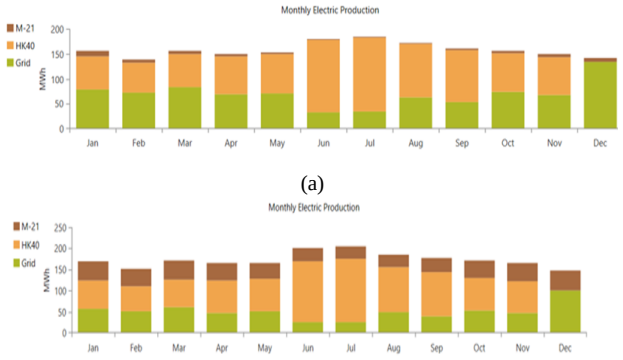

(a)

(b)

Fig. 15. Annual average output, operational hours, and power production for the proposed scenarios at Buffels Bay

Fig. 19 and Fig. 20 illustrate the energy generation portfolio is as follows: wind turbines generate 465,822 kWh/year, accounting for 22% of the total energy output; the 40-kW generic hydrokinetic system produces 1,003,094 kWh/year, representing 48%; and grid purchases add 608,805 kWh/year, constituting 29.3% of the energy mix. In total, the system generates 2,077,721 kWh/year, resulting in 17,548 kWh/year of excess electricity. This leads to a cumulative surplus of 367,925 kWh/year. These results highlight the system's capability to efficiently meet energy demands while maintaining a significant surplus, demonstrating its effectiveness in integrating renewable energy sources.

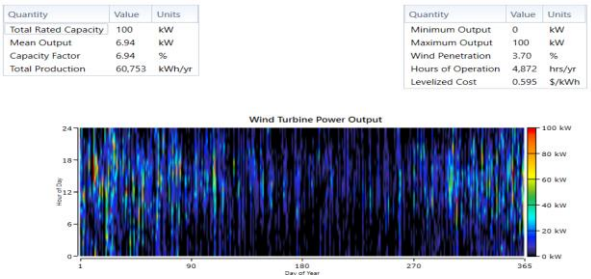

Fig. 16.Wind turbine power output

The wind turbine system, with a total rated capacity of 100 kW, has an average output of 6.94 kW and a capacity factor of 6.94%, indicating that it operates below its maximum potential most of the time. The system generates 60,753 kWh per year, with a wide range of outputs from 0 kW to its maximum of 100 kW. The wind penetration of 3.70% shows a modest contribution to the overall energy mix. Operating for 4,872 hours annually, the system provides intermittent power. However, the

levelized cost of energy (LCOE) at $0.595 per kWh is relatively high, suggesting that the system is not cost-competitive compared to other renewable energy sources.

Quantity	Value	Units
Total Rated Capacity	200	kW
Mean output	115	kW
Capacity factor	57.3	%
Total Production	1,003,094	kWh/yr

Quantity	Value	Units
Minimum output	0	kW
Maximum output	200	kW
Hydrokinetic penetration	61.1	%
Hours of operation	8,016	hr/yr
Levelized Cost	0.00957	$/kWh

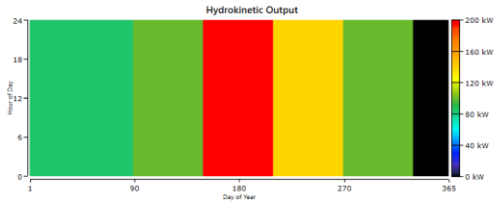

Fig. 17. Hydrokinec Output

Energy needs are crucial for enhancing overall efficiency.

The HOMER Pro results reveal the following:

- **AC Primary Load:** Consumes 1,642,500 kWh/year, making up 89.7% of total consumption. This suggests AC loads are the main energy consumers in the system.
- **DC Primary Load and Deferrable Load:** No consumption is reported for these, indicating they are either not utilized or negligible
- **Grid Sales:** The system sells 187,853 kWh/year back to the grid, representing 10.3% of total consumption. This helps balance the energy load and provides potential revenue.

Implications: The high AC load consumption highlights its importance. The lack of DC or deferrable loads might suggest they are not needed. Effective management of AC loads and leveraging grid sales can enhance overall system efficiency and performance.

The cost summary in Fig. 22 reveals that the Generic Hydrokinetic (40 kW) system has the highest total net present cost (NPC) of $890,133 due to substantial capital, operating, and replacement costs. The Grid incurs operational expenses amounting to $712,205. The XANT M-21 (100 kW wind turbine), with a total NPC of $417,817, also reflects significant capital and replacement costs. The lead-acid battery and system converter contribute relatively lower NPCs of $2,053 and $71,764, respectively. Overall, the hybrid system's total NPC is $2.09 million, indicating a need for cost optimization to improve economic viability. The simulation details the cost allocation for each component, broken down into capital cost, replacement cost, operation and maintenance cost, and salvage value in Table V. A negative salvage value indicates no residual value at the project's end.

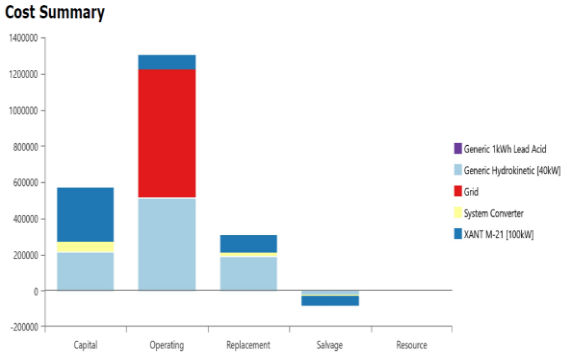

Fig. 22. Cost Summary

The net present cost (NPC) analysis in Fig. 23 provides a comprehensive overview of the economic impact of various components in the hybrid energy system. The Generic Hydrokinetic (40 kW) system shows the highest total NPC at $890,133, driven mainly by its high operating costs ($511,334) and replacement costs ($187,963). The Grid contributes significantly to overall costs, with a substantial NPC of $785,512 entirely due to operating expenses. The System Converter has a relatively lower NPC of $61,061, with notable contributions from capital costs ($45,581) and replacement costs ($19,019). Overall, the total system NPC is $1.74 million, indicating the need for strategies to minimize costs, especially in operating and replacement expenditures, to enhance the system's economic feasibility.

The DCCFs over 25 years in Fig. 24 shows a substantial initial value of $12,000,000, indicating strong early performance. However, this value decreases significantly to $1,000,000 and eventually to $0, reflecting declining cash flows or increasing costs over time. The trend suggests that while the project was initially profitable, its long-term financial viability is in

question. This decline necessitates a review of financial strategies and operational efficiency to address the decreasing returns and manage risks effectively. Investors should consider these trends when making decisions about ongoing investment or project adjustments.

TABLE V
PRESENT COSTS

Component	Capital($)	Replacement ($)	0&M($)	Fuel ($)	Salvage ($)	Total($)
Gen Hydro (40kw)	70,000.00	60,913.97	0.00	0.00	8,154.95	122,759.01
Grid	0.00	0.00	816,533.04	0.00	0.00	816,533.04

System Converter	59,003.14	24,619.95	0.00	0.00	4,582.55	79,040.54
System	126,958.00	887,682.00	0.00	0.00	12,579.00	1.09M

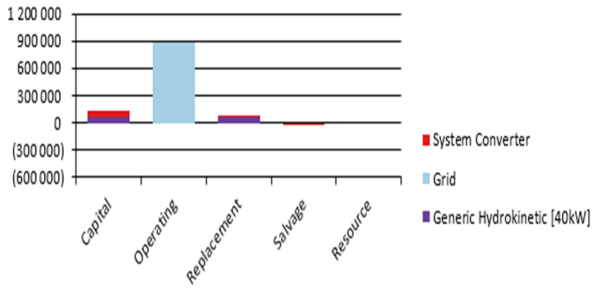

Fig. 18. Net Present Cost analysis

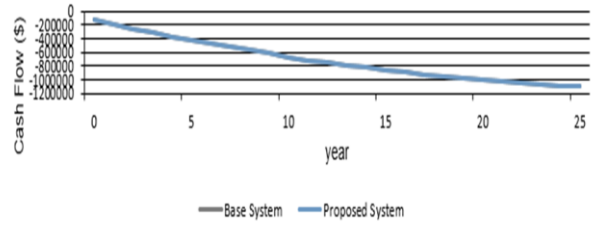

Fig. 19. Cumulative Discounted Cash Flows

B. Environmental Impact

The tidal and wind grid-connected system emits 399,999 kg/year of CO_2, which, while lower than fossil fuels, still represents a significant greenhouse gas footprint. Notably, there are no emissions of carbon monoxide, unburned hydrocarbons, or particulate matter, which is beneficial for air quality. However, the system produces 1,734 kg/year of sulfur dioxide (SO_2) and 848 kg/year of nitrogen oxides (NO_x) indicated in Table VI. While these levels are relatively low, they can contribute to environmental issues such as acid rain and smog. Continuous efforts to minimize CO_2, SO_2, and NO_x emissions are crucial for improving the system's overall sustainability.

TABLE VI
POLLUTANT EMISSIONS

Quantity	Value	Units
Carbon Dioxide	399,999	Kg/yr
Carbon Monoxide	0	Kg/yr
Unburned Hydrocarbons	0	Kg/yr
Particulate Matter	0	Kg/yr
Sulphur Dioxide	1,734	Kg/yr
Nitrogen Oxides	848	Kg/yr

IV. Conclusion

This study explores the feasibility and advantages of a grid-connected offshore wind and tidal storage power system in Buffels Bay. By using HOMER Pro software, the optimized model reveals substantial cost savings and environmental benefits, making it a valuable example for similar renewable energy projects in coastal regions. The research focused on a DC-linked wind-tidal battery-grid system in South Africa, leveraging the area's abundant wind and tidal resources to design an efficient and eco-friendly microgrid.

Simulations were conducted to develop a DC-linked microgrid that integrates seamlessly with the national grid to supply residential loads in Buffels Bay, Cape Town. The design utilized data on wind speeds and tidal currents to evaluate capacity and cost-effectiveness.

Key findings include:

- **Tidal Power:** Tidal currents can generate electricity for 69.3% of the year, providing a reliable energy source.
- **Wind Power:** Wind speeds are insufficient for electricity generation 78.2% of the year, highlighting the need for optimization.
- **Microgrid Integration:** The proposed design enables DC power from Buffels Bay to be efficiently integrated into the national grid. This involves installing wind and tidal turbines on a single offshore platform, connecting them to a DC-linked system, and transmitting power through a DC marine cable to an onshore DC-AC converter, followed by transmission via an AC land cable to the utility grid station.

The integration of offshore renewable sources, as demonstrated by HOMER Pro, shows strong potential for meeting energy demands. Combining wind and tidal power into a hybrid system offers distinct advantages: tidal energy provides a stable and predictable base load, while wind turbines can boost energy production when wind conditions are favourable. This hybrid approach mitigates the intermittency and variability typically associated with wind energy, enhancing the system's overall reliability. However, the relatively low wind energy contribution and high levelized cost of energy (LCOE) from wind indicate areas for potential improvement. Strategies such as better turbine placement or the adoption of more efficient technologies could enhance wind energy production and reduce costs. Expanding the tidal component or optimizing its integration with wind could further improve the hybrid system's efficiency and cost-effectiveness. In conclusion, the hybrid system effectively balances the variability of wind power with the stability of tidal energy, resulting in a robust renewable energy solution. To maximize the potential of this system, it is crucial to optimize both

components, ensuring economic viability and a reliable energy supply.

Acknowledgements

The authors would like to express their gratitude to the Cape Peninsula University of Technology (CPUT) for providing comprehensive support and resources for this research.

Conflict of Interest

The authors declare that they have no known competing financial interests or personal relationships that could have appeared to influence the work reported in this paper.

Author Contributions

Author 1 was responsible for the design and simulation of the HOMER Pro model and took the lead in authoring the methodology and results sections of the paper. Author 2 concentrated on optimizing the model, designing the input parameters, overseeing data collection, and managing the site selection process. Meanwhile, Author 3 contributed by assisting in the design of input parameters, handling data collection, and writing the discussion and conclusion sections. Each author played a critical role in different aspects of the research, ensuring a comprehensive and collaborative effort.

References

[1] M. Bazilian *et al.*, "Energy access scenarios to 2030 for the power sector in sub-Saharan Africa," *Util. Policy*, vol. 20, no. 1, pp. 1–16, 2012, doi: 10.1016/j.jup.2011.11.002.

[2] Sanedi and Promethium Carbon, "Appraisal of Implementation of Fossil Fuel and Renewable Energy Hybrid Technologies in South Africa," 2017. [Online]. Available: https://www.sanedi.org.za/img/wp-content/uploads/2018-01-15 Hybrid Technologies in South Africa full report.pdf.

[3] E. L. Meyer and O. K. Overen, "Towards a sustainable rural electrification scheme in South Africa : Analysis of the Status quo," *Energy Reports*, vol. 7, no. 2021, pp. 4273–4287, 2025, doi: 10.1016/j.egyr.2021.07.007.

[4] M. Kamali Saraji and D. Streimikiene, "Challenges to the low carbon energy transition: A systematic literature review and research agenda," *Energy Strateg. Rev.*, vol. 49, no. August, p. 101163, 2023, doi: 10.1016/j.esr.2023.101163.

[5] T. M. I. Riayatsyah, T. A. Geumpana, I. M. Rizwanul Fattah, S. Rizal, and T. M. Indra Mahlia, "Techno-Economic Analysis and Optimisation of Campus Grid-Connected Hybrid Renewable Energy System Using HOMER Grid," *Sustain.*, vol. 14, no. 13, 2022, doi: 10.3390/su14137735.

[6] O. J. Ayamolowo, P. T. Manditereza, and K. Kusakana, "South Africa power reforms: The Path to a dominant renewable energy-sourced grid," *Energy Reports*, vol. 8, pp. 1208–1215, 2022, doi: 10.1016/j.egyr.2021.11.100.

[7] A. A. Kebede *et al.*, "Techno-economic analysis of lithium-ion and lead-acid batteries in stationary energy storage application," *J. Energy Storage*, vol. 40, no. June, p. 102748, 2021, doi: 10.1016/j.est.2021.102748.

[8] J. Li, G. Wang, Z. Li, S. Yang, W. T. Chong, and X. Xiang, "A review on development of offshore wind energy conversion system," *Int. J. Energy Res.*, vol. 44, no. 12, pp. 9283–9297, 2020, doi: 10.1002/er.5751.

[9] D. Wu *et al.*, "Grid Integration of Offshore Wind Power: Standards, Control, Power Quality and Transmission," *IEEE Open J. Power Electron.*, vol. 5, no. April, pp. 583–604, 2024, doi: 10.1109/OJPEL.2024.3390417.

[10] A. Uihlein and D. Magagna, "Wave and tidal current energy – A review of the current state of research beyond technology," *Renew. Sustain. Energy Rev.*, vol. 58, pp. 1070–1081, 2016, doi: 10.1016/j.rser.2015.12.284.

[11] K. Maalawi, *Modeling, Simulation and Optimization of Wind Farms and Hybrid Systems*. 2020.

[12] Y. Shirai, S. Minamoto, K. Yonemura, and M. L. Rahman, "Output power control of hybrid off-shore-wind and tidal turbine generation system with battery storage system," *19th Int. Conf. Electr. Mach. Syst. ICEMS 2016*, pp. 1–6, 2017.

[13] M. L. Rahman, S. Oka, and Y. Shirai, "Hybrid power generation system using offshore-wind turbine and tidal turbine for power fluctuation compensation (HOT-PC)," *IEEE Trans. Sustain. Energy*, vol. 1, no. 2, pp. 92–98, 2010, doi: 10.1109/TSTE.2010.2050347.

[14] E. Hu *et al.*, "Research on capacity optimization of offshore wind power flow combined power generation system based on homer," *2020 IEEE 4th Conf. Energy Internet Energy Syst. Integr. Connect. Grids Towar. a Low-Carbon High-Efficiency Energy Syst. EI2 2020*, pp. 2684–2689, 2020, doi: 10.1109/EI250167.2020.9346843.

[15] D. Lande-Sudall, T. Stallard, and P. Stansby, "Co-located offshore wind and tidal stream turbines: Assessment of energy yield and loading," *Renew. Energy*, vol. 118, no. April, pp. 627–643, 2018, doi: 10.1016/j.renene.2017.10.063.

[16] N. M. Nasab, J. Kilby, and L. Bakhtiaryfard, "The Potential for Integration of Wind and Tidal Power in New Zealand," pp. 1–21, 2020.

[17] T. Ma, C. R. Lashway, Y. Song, and O. Mohammed, "Optimal renewable energy farm and energy storage sizing method for future hybrid power system," *2014 17th Int. Conf. Electr. Mach. Syst. ICEMS 2014*, pp. 2827–2832, 2014, doi: 10.1109/ICEMS.2014.7013979.

[18] M. F. Zia, M. Nasir, E. Elbouchikhi, M. Benbouzid, J. C. Vasquez, and J. M. Guerrero, "Energy management system for a hybrid PV-Wind-Tidal-Battery-based islanded DC microgrid: Modeling and experimental validation," *Renew. Sustain. Energy Rev.*, vol. 159, no. June 2021, p. 112093, 2022, doi: 10.1016/j.rser.2022.112093.

[19] A. F. Minai, M. A. Husain, M. Naseem, and A. A. Khan, "Please mail to for full paper .," no. July, 2021, doi: 10.1515/ijeeps-2021-0085.

[20] K. A. Kavadias, "Hybrid Renewable Energy Systems ' Optimisation . A Review and Extended Comparison of the Most-Used Software Tools," 2021.

[21] K. S. Krishna and K. S. Kumar, "A review on hybrid renewable energy systems," vol. 52, pp. 907–916, 2015, doi: 10.1016/j.rser.2015.07.187.

[22] B. Astrid, M. Nouadje, P. Tiam, and V. Chegnimonhan, "Techno-economic analysis of an islanded energy system based on geothermal / biogas / wind / PV utilizing battery technologies : A case study of Woulde , Adamawa ' s region , Cameroon," vol. 54, no. June, 2024, doi: 10.1016/j.esr.2024.101469.

[23] Y. Sahri *et al.*, "Energy management system for hybrid PV/wind/battery/fuel cell in microgrid-based hydrogen and economical hybrid battery/super capacitor energy storage," *Energies*, vol. 14, no. 18, 2021, doi: 10.3390/en14185722.

[24] F. Ghayoor, A. G. Swanson, and H. Sibanda, "Optimal sizing for a grid-connected hybrid renewable energy system: A case study of the residential sector in Durban, South Africa," *J. Energy South. Africa*, vol. 32, no. 4, pp. 11–27, 2021, doi: 10.17159/2413-3051/2021/v32ia8362.

[25] S. Abdelhady, D. Borello, and S. Santori, "Economic feasibility of small wind turbines for domestic consumers in Egypt based on the new Feed-in Tariff," *Energy Procedia*, vol. 75, pp. 664–670, 2015, doi: 10.1016/j.egypro.2015.07.482.

[26] Q. Hassan, S. Algburi, A. Zuhair, H. M. Salman, and M. Jaszczur,

"Results in Engineering Review article A review of hybrid renewable energy systems : Solar and wind-powered solutions : Challenges , opportunities , and policy implications," *Results Eng.*, vol. 20, no. November, p. 101621, 2023, doi: 10.1016/j.rineng.2023.101621.

[27] S. Saha, G. Saini, S. Mishra, A. Chauhan, and S. Upadhyay, "A comprehensive review of techno-socio-enviro-economic parameters, storage technologies, sizing methods and control management for integrated renewable energy system," *Sustain. Energy Technol. Assessments*, vol. 54, no. November, p. 102849, 2022, doi: 10.1016/j.seta.2022.102849.

[28] B. Bhandari, K. T. Lee, G. Y. Lee, Y. M. Cho, and S. H. Ahn, "Optimization of hybrid renewable energy power systems: A review," *Int. J. Precis. Eng. Manuf. - Green Technol.*, vol. 2, no. 1, pp. 99–112, 2015, doi: 10.1007/s40684-015-0013-z.

[29] A. Bayu, D. Anteneh, and B. Khan, "Grid Integration of Hybrid Energy System for Distribution Network," *Distrib. Gener. Altern. Energy J.*, vol. 37, no. 3, pp. 537–556, 2022, doi: 10.13052/dgaej2156-3306.3738.

[30] B. Jiang, H. Lei, W. Li, and R. Wang, "A novel multi-objective evolutionary algorithm for hybrid renewable energy system design," *Swarm Evol. Comput.*, vol. 75, no. February, p. 101186, 2022, doi: 10.1016/j.swevo.2022.101186.

[31] A. N. Abdalla *et al.*, "Integration of energy storage system and renewable energy sources based on artificial intelligence: An overview," *J. Energy Storage*, vol. 40, no. April, p. 102811, 2021, doi: 10.1016/j.est.2021.102811.

[32] M. Usama *et al.*, "A comprehensive review on protection strategies to mitigate the impact of renewable energy sources on interconnected distribution networks," *IEEE Access*, vol. 9, pp. 35740–35765, 2021, doi: 10.1109/ACCESS.2021.3061919.

[33] S. Twaha and M. A. M. Ramli, "A review of optimization approaches for hybrid distributed energy generation systems: Off-grid and grid-connected systems," *Sustain. Cities Soc.*, vol. 41, no. May, pp. 320–331, 2018, doi: 10.1016/j.scs.2018.05.027.

[34] T. Hirose and H. Matsuo, "Standalone Hybrid Wind-Solar Power Generation System Applying Dump Power Control Without Dump Load," *IEEE Trans. Ind. Electron.*, vol. 59, no. 2, pp. 988–997, 2012, doi: 10.1109/TIE.2011.2159692.

[35] B. Modu, P. Abdullah, and A. Lawan, "ScienceDirect A systematic review of hybrid renewable energy systems with hydrogen storage : Sizing , optimization , and energy management strategy," *Int. J. Hydrogen Energy*, vol. 48, no. 97, pp. 38354–38373, 2023, doi: 10.1016/j.ijhydene.2023.06.126.

[36] D. Suchitra, R. Rajarajeswari, and J. Dasgupta, "Optimization of hybrid renewable energy system using homer," *Int. J. Recent Technol. Eng.*, vol. 8, no. 2 Special Issue 11, pp. 2542–2550, 2019, doi: 10.35940/ijrte.B1301.0982S1119.

[37] D. Jackson and T. Persoons, "Feasibility Study and Cost-Benefit Analysis of Tidal Energy : A Case Study for Ireland," no. May 2002, pp. 1–6, 2012.

[38] M. C. Sousounis, J. K. H. Shek, and M. A. Mueller, "Filter design for cable overvoltage and power loss minimization in a tidal energy system with onshore converters," *IEEE Trans. Sustain. Energy*, vol. 7, no. 1, pp. 400–408, 2016, doi: 10.1109/TSTE.2015.2424258.

[39] J. Bao, W. Bao, and J. Gong, "A PWM Multilevel Current-Source Inverter Used for Grid-Connected Wind Energy Conversion System," *Energy Procedia*, vol. 16, pp. 461–466, 2012, doi: 10.1016/j.egypro.2012.01.075.

[40] F. Oloo, B. Molefyane, and M. Rampokanyo, "Modelling and optimisation studies for generator dispatch strategies for deployment of an off-grid micro-grid in South Africa," *6th IEEE Int. Energy Conf. ENERGYCon 2020*, pp. 533–538, 2020, doi: 10.1109/ENERGYCon48941.2020.9236547.

[41] V. Ani, "Sizing application for the development of an integrated PV/wind/hydro-battery energy system for sustainable power supply," *Sustain. Eng. Innov.*, vol. 4, no. 2, pp. 127–145, 2022, doi: 10.37868/sei.v4i2.id156.

[42] M. Shehzad and F. Gueniat, "Optimal operation of renewable energy microgrids considering lifetime characteristics of battery energy storage system," *Proc. IEEE Conf. Decis. Control*, vol. 2021-Decem, no. 4, pp. 4958–4963, 2021, doi: 10.1109/CDC45484.2021.9683478.

[43] J. Verma and D. Kumar, "Recent developments in energy storage systems for marine environment," *Mater. Adv.*, vol. 2, no. 21, pp. 6800–6815, 2021, doi: 10.1039/d1ma00746g.

[44] L. M. Fernandez, P. Garcia, C. A. Garcia, and F. Jurado, "Hybrid electric system based on fuel cell and battery and integrating a single dc/dc converter for a tramway," *Energy Convers. Manag.*, vol. 52, no. 5, pp. 2183–2192, 2011, doi: 10.1016/j.enconman.2010.12.028.

[45] C. Rautenbach, M. A. Barnes, and M. de Vos, "Tidal characteristics of South Africa," *Deep. Res. Part I Oceanogr. Res. Pap.*, vol. 150, no. February, p. 103079, 2019, doi: 10.1016/j.dsr.2019.103079.

[46] S. Rehman, N. Natarajan, M. A. Mohandes, J. P. Meyer, M. M. Alam, and L. M. Alhems, "Wind and wind power characteristics of the eastern and southern coastal and northern inland regions, South Africa," *Environ. Sci. Pollut. Res.*, vol. 29, no. 57, pp. 85842–85854, 2022, doi: 10.1007/s11356-021-14276-9.

[47] G. Prinsloo, R. Dobson, and A. Brent, "Scoping exercise to determine load profile archetype reference shapes for solar co-generation models in isolated off-grid rural African villages," *J. Energy South. Africa*, vol. 27, no. 3, pp. 11–27, 2016, doi: 10.17159/2413-3051/2016/v27i3a1375.

[48] M. L. Rahman, K. Nishimura, K. Motobayashi, S. Fujioka, and Y. Shirai, "Characteristic of small-scale BESS for HOTT generation system," *Dig. Tech. Pap. - InnoTek 2014 2014 IEEE Innov. Technol. Conf.*, pp. 1–9, 2014, doi: 10.1109/InnoTek.2014.6877363.

[49] K. Foysal Haque, N. Saqib, and M. S. Rahman, "An optimized stand-alone green hybrid grid system for an offshore Island, Saint Martin, Bangladesh," *Int. Conf. Energy Power Eng. Power Progress, ICEPE 2019*, 2019, doi: 10.1109/CEPE.2019.8726596.

[50] L. B. Navid Majdi, Jeff Kilby, "Case study of a hybrid wind and tidal turbines system with a microgrid for power supply to a remote off-grid community in New Zealand," *Energies*, vol. 14, no. 12, 2021, doi: 10.3390/en14123636.

[51] T. M. I. Riayatsyah, T. A. Geumpana, and I. M. R. Fattah, "Techno-Economic Analysis of Hybrid Diesel Generators and Renewable Energy for a Remote Island in the Indian Ocean Using HOMER Pro," 2022.

[52] R. George, A. Al-hinai, R. Al-abri, and A. Malik, "Optimization and techno-economic analysis of PV / Battery system for street lighting using genetic algorithm – A case study in Oman," *Clean. Eng. Technol.*, vol. 8, no. February, p. 100475, 2022, doi: 10.1016/j.clet.2022.100475.

[53] S. Toumi, Y. Amirat, E. Elbouchikhi, Z. Zhou, and M. Benbouzid, "Techno-Economic Optimal Sizing Design for a Tidal Stream Turbine – Battery System," 2023.